metabolites

MDPI

Article

Guanosine Prevents Spatial Memory Impairment and Hippocampal Damage Following Amyloid-$\beta_{1–42}$ Administration in Mice

Victor Coelho [1,†], Luisa Bandeira Binder [1,†], Naiani Ferreira Marques [2], Leandra Celso Constantino [1], Gianni Mancini [2,3,*] and Carla Inês Tasca [1,2,3,*]

1 Programa de Pós-Graduação em Neurociências, Centro de Ciências Biológicas, Universidade Federal de Santa Catarina, Florianópolis 88040, Brazil
2 Programa de Pós-Graduação em Bioquímica, Centro de Ciências Biológicas, Universidade Federal de Santa Catarina, Florianópolis 88040, Brazil
3 Departamento de Bioquímica, Centro de Ciências Biológicas, Universidade Federal de Santa Catarina, Florianópolis 88040, Brazil
* Correspondence: gianni.mancini@gmail.com (G.M.); carla.tasca@ufsc.br (C.I.T.)
† These authors contributed equally to this work.

Abstract: Alzheimer's disease (AD) is a progressive neurodegenerative illness responsible for cognitive impairment and dementia. Accumulation of amyloid-beta (Aβ) peptides in neurons and synapses causes cell metabolism to unbalance, and the production of reactive oxygen species (ROS), leading to neuronal death and cognitive damage. Guanosine is an endogenous nucleoside recognized as a neuroprotective agent since it prevents glutamate-induced neurotoxicity by a mechanism not yet completely elucidated. In this study, we evaluated behavioral and biochemical effects in the hippocampus caused by the intracerebroventricular (i.c.v.) infusion of $A\beta_{1–42}$ peptide (400 pmol/site) in mice, and the neuroprotective effect of guanosine (8 mg/kg, i.p.). An initial evaluation on the eighth day after $A\beta_{1–42}$ infusion showed no changes in the tail suspension test, although ex vivo analyses in hippocampal slices showed increased ROS production. In the second protocol, on the tenth day following $A\beta_{1–42}$ infusion, no effect was observed in the sucrose splash test, but a reduction in the recognition index in the object location test showed impaired spatial memory. Analysis of hippocampal slices showed no ROS production and mitochondrial membrane potential alteration, but a tendency to increase glutamate release and a significant lactate release, pointing to a metabolic alteration. Those effects were accompanied by decreased cell viability and increased membrane damage. Guanosine treatment prevented behavioral and biochemical alterations evoked by $A\beta_{1–42}$, suggesting a potential role against behavioral and biochemical damage evoked by Aβ in the hippocampus.

Keywords: Alzheimer's disease; guanosine; $A\beta_{1–42}$; glutamate; hippocampus

Citation: Coelho, V.; Binder, L.B.; Marques, N.F.; Constantino, L.C.; Mancini, G.; Tasca, C.I. Guanosine Prevents Spatial Memory Impairment and Hippocampal Damage Following Amyloid-$\beta_{1–42}$ Administration in Mice. *Metabolites* **2022**, *12*, 1207. https://doi.org/10.3390/metabo12121207

Academic Editor: Wolfgang Bogner

Received: 21 October 2022
Accepted: 28 November 2022
Published: 1 December 2022

1. Introduction

Alzheimer's disease (AD) is a progressive and irreversible illness involving a severe disturbance in memory and cognition, which inevitably results in the need for intensive care [1,2]. Amyloid-beta (Aβ) is a proteolytic fragment formed from the cleavage of the amyloid precursor protein (APP), a transmembrane glycoprotein. The formation of 40 to 42 amino acids Aβ peptides in their oligomeric and/or fibrillar forms leads to their accumulation and these, in turn, promote neurotoxicity [3]. Synaptic and mitochondrial dysfunctions are observed both in transgenic AD models [4] and in models that mimic the early stages of AD, obtained through intracerebroventricular (i.c.v.) infusion of Aβ peptides [5]. Although acute Aβ infusion does not trigger all the pathological features of AD, i.c.v. $A\beta_{1–40}$ infusion induces inflammatory responses, and decreases brain-derived neurotrophic factor (BDNF) levels. Additionally, it causes oxidative stress and changes in glutamatergic transmission in the hippocampus that may be associated with cognitive

impairment in learning and memory, and in depressive-like behaviour in mice [6–10]. However, $A\beta_{1–42}$ was identified as the most neurotoxic and prevalent in the central nervous system (CNS) in severe cases of AD and during disease progression [11]. Therefore, our aim was to evaluate the effect of a neuroprotective strategy on early events of $A\beta_{1–42}$-induced hippocampal toxicity.

Guanosine (GUO) is an endogenous guanine nucleoside that acts as an intercellular signalling molecule affecting multiple neural processes [12–14]. Guanosine can be released to the extracellular milieu from astrocytes by nucleoside transporters [15], or it is produced in the extracellular space by guanine nucleotide metabolism via membrane-bound ectonucleotidases activity [16]. In ischemic or hypoxic insults, guanosine levels increase [17], and it has been suggested to act as a glutamatergic transmission modulator [14,18], thus reducing excitotoxicity. Guanosine has been shown to exert neuroprotective effects, such as preventing ischemic brain damage [19,20]; prevention of behavioral deficits and mitochondrial dysfunction in traumatic brain injuries [21,22]; prevention of memory deficits; and prevention of anhedonic-like behavior and loss of mitochondrial Ca^{2+} homeostasis induced by Aβ peptides [6,23]. Additionally, guanosine exerts an antidepressant-like effect in mice [13].

Of fundamental importance, guanosine shows several physiological effects, such as neurotrophic [24,25] and neurogenic [26], and favours antioxidant balance [22]. Guanosine was able to effectively decrease ROS levels, reduce mitochondrial swelling, and prevent mitochondrial membrane potential collapse in hippocampal slices subjected to oxygen-glucose deprivation [20].

Here we evaluated guanosine effects in an in vivo AD murine model assessing cell viability, oxidative, metabolic, and behavioural alterations during early events of $A\beta_{1–42}$-induced hippocampal toxicity. The current study was the first to evaluate guanosine protective effects following 8 and 10 days of $A\beta_{1–42}$ peptide i.c.v. infusion. Guanosine prevents alteration in the locomotor activity and the increased hippocampal ROS generation caused by $A\beta_{1–42}$ (on the 8th day). Guanosine is also effective in preventing $A\beta_{1–42}$-induced impairment in the hippocampal-dependent short-term spatial memory, increased damage to hippocampal slices, and metabolic alterations as increased lactate release (on the 10th day). Guanosine treatment prevented behavioural and biochemical alterations evoked by $A\beta_{1–42}$.

2. Materials and Methods

2.1. Animals

Adult male Swiss mice (3 months old/40–50 g) provided by the animal facility from Universidade Federal de Santa Catarina (UFSC) were maintained in a 12-h cycle light/dark at 22 ± 1 °C (light phase started at 7:00 a.m.) in housing boxes (10 animals per box) with water and food ad libitum. Once received from the animal facility, mice were accommodated in the room for 10 days before experiments for acclimation. Animals were randomly selected from their housing boxes and allocated to treatment groups. The experimental procedures performed in this study followed "The ARRIVE Guidelines" published in 2010 and were approved by the Ethical Committee for Animal Research (CEUA/UFSC PP00955). Behavioral experiments started in the morning (8:00 a.m.). Animals were acclimatized with the handler before the beginning of the treatments to reduce stress. All experiments were designed to reduce the suffering and number of animals used. The study was not pre-registered, and no blinding was performed.

2.2. Drugs

Human $A\beta_{1–42}$ (Tocris, Bristol, UK) was diluted in 0.1 M phosphate-buffered saline (PBS) in a stock solution (1 mg/mL) and then aggregated at 37 °C for 4 days and aliquots were stored at −20 °C. Guanosine (Sigma-Aldrich Brasil Ltda, Cat# G6752, Sao Paulo, Brazil) was freshly dissolved in saline (NaCl 0.9%) to 8 mg/kg (i.p.).

2.3. Amyloid-Beta Infusion

The aggregated form of amyloid-$\beta_{1–42}$ ($A\beta_{1–42}$) peptide (400 pmol/3 µL site) or PBS (3 µL/site) was administered intracerebroventricular (i.c.v.) according to [10]. Mice were briefly anesthetized with isoflurane 0.96% (0.75 CAM; Instituto BioChimico®, Rio de Janeiro, Brazil) using a vaporizing system (Isoflurane Vaporizer HB 4.3, HB Hospitalar Indústria e Comércio®, Sao Paulo, Brazil) and then gently retained by hand for the i.c.v administration. Under mild anaesthesia (only sufficient for loss of postural reflex), the needle was introduced unilaterally, not more than 2 mm into the brain, 1 mm to the right of the median point of each eye, and 1 mm posterior to a line drawn through the anterior base of the eye (used as an external reference). The exact location of the injection site was only confirmed at the time of dissection or euthanasia of the animals. No incorrect infusion was detected, and all mice results were included in the statistical analysis.

2.4. Experimental Design

To study the effects of guanosine on the molecular changes induced by $A\beta_{1–42}$, animals were treated intraperitoneally (i.p.) with guanosine 8 mg/kg per day. On the first day, guanosine was administered 30 min after the i.c.v. infusion of $A\beta_{1–42}$ or PBS, and treatment was carried out daily [10]. Control animals were treated with the vehicle saline (NaCl 0.9%; i.p.) for the same period. The treatment was carried out by the administration of 10 uL/g weight of the animal, both for guanosine and saline solutions. This study evaluated two-time courses of early $A\beta_{1–42}$-induced neurotoxicity effects and guanosine modulation on behavioural and biochemical parameters: a first experimental group (Protocol 1) was analysed on day 8 following $A\beta_{1–42}$ infusion and daily guanosine treatment (Figure 1A); and a second experimental group (Protocol 2) was analysed on day 10 following $A\beta_{1–42}$ infusion and daily guanosine treatment (Figure 1B).

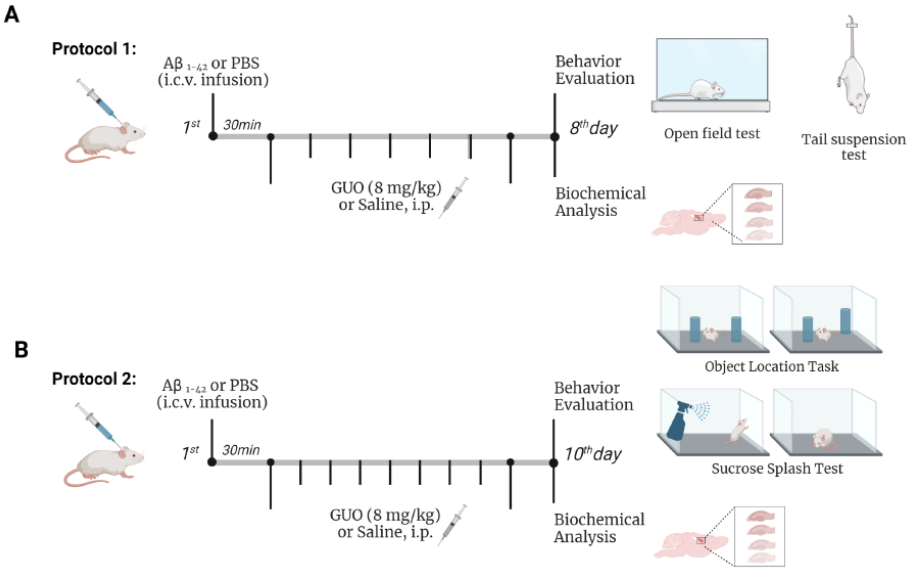

Figure 1. Overview of experimental protocols for behavioural and biochemical analysis in mice following $A\beta_{1–42}$ i.c.v. infusion and guanosine treatment. Protocol 1: Mice were subjected to intracerebroventricular (i.c.v.) infusion of $A\beta_{1–42}$ (400 pmol/3 uL site) or phosphate-buffered saline (PBS) infusion, and after 30 min received an intraperitoneal (i.p.) treatment of guanosine (GUO, 8 mg/kg) for 7 days. On the eighth day, mice were subjected to the open field test and to the tail suspension test, euthanized, and hippocampal slices assessed for ROS production and slice viability (MTT reduction and PI incorporation) (**A**). Protocol 2: On the tenth day after treatments, mice were subjected to the sucrose splash test and to the object location test. Animals were euthanized and hippocampal slices were assessed for ROS production, mitochondrial membrane potential, glutamate and lactate efflux, and slice viability (**B**).

2.5. Behavioral Analysis

Mice subjected to Protocol 1 were tested for depressive-like behavior in the tail suspension test (TST) followed by the open field test (OFT) on day 8 following treatments (Figure 1A). In Protocol 2, independent animal cohorts were tested for anhedonic-like behavior or short-term spatial memory, assessed in the sucrose-splash test (SST), and in the object relocation test (ORT), respectively, at the day 10 following treatments (Figure 1B). Behavioral tests were carried out between 8:00 a.m. and noon, and they were scored by the same rater in an observation sound-attenuated room under low-intensity light (12 lux), where the mice had been habituated for at least 1 h before the beginning of the tests. Behavior was monitored through a video camera positioned above the apparatuses, and the videos were later analyzed with the ANYMaze® (Stoelting Co., Wood Dale, IL, USA) video tracking system. The apparatus was cleaned with 10 % ethanol between animals to avoid odor clues.

2.6. Tail Suspension Test (TST)

Animals were subjected to TST, according to [27]. Mice both acoustically and visually isolated were suspended 50 cm above the floor by their tails with adhesive tape and placed approximately 1 cm from the tip of the tail. The total duration of mice immobility time induced by tail suspension was measured for 6 min [28].

2.7. Open-Field Test (OFT)

To assess the locomotor activity in order to ensure an antidepressant-like effect instead of an alteration of locomotor activity, mice were subjected to OFT after the TST. The apparatus consisted of a wooden box measuring 40 × 60 × 50 cm. The floor of the arena was divided into 12 equal squares. The number of squares crossed with all paws (crossings) was recorded for 6 min [29].

2.8. Sucrose Splash Test (SST)

On the 10th day following treatment, animals were subjected to the sucrose splash test, carried out as previously described [6]. SST consisted of sprayings a 10% sucrose solution on the dorsal coat of a mouse placed individually in clear Plexiglas boxes (9 × 7 × 11 cm). After applying sucrose solution, the latency and time spent grooming were recorded for a period of 5 min. The apparatuses were cleaned with a solution of 10 % ethanol between tests to hide the animal's clues.

2.9. Object Location Task (OLT)

The short-term spatial memory of mice was assessed using the object location task as described [6]. The task consisted of two 5 min sessions (training and test) separated by a 90 min interval. In the training session, mice were placed in the center of the open field with two identical objects for 5 min, and object exploration was recorded using a stopwatch when mice sniffed, whisked, or looked at the objects from no more than 1 cm away. After 90 min, one object was moved to a new location, and the time spent by the animals exploring the objects in new (moved) and initial (familiar) locations was recorded over 5 min (test session). Objects were thoroughly cleaned with 10 % ethanol after each trial to minimize the presence of olfactory trails. To analyze the cognitive performance, a discrimination index of location was calculated as (T moved × 100)/(T moved + T familiar), where T moved is the time spent exploring the displaced object and T familiar is the time spent exploring the non-displaced object.

2.10. Biochemistry Analysis

2.10.1. Preparation of Brain Slices

On the 8th (protocol 1, Figure 1A) or 10th day (protocol 2, Figure 1B) following treatments, animals were euthanized by decapitation and the whole brain was quickly removed and placed on an ice-cold wetted plate. Hippocampi were rapidly dissected in ice-cold Krebs-Ringer Buffer (KRB, composition in millimolar: NaCl 122, KCl 3, $MgSO_4$1.2, $CaCl_2$1.3, KH_2PO_4 0.4, $NaHCO_3$ 25, and D-glucose 10, bubbled with 95% CO_2/5% O_2 up to pH 7.4). Hippocampi were sliced (0.4 mm) using a McIlwain Tissue Chopper (The Mickle Laboratory Engineering Co., Ltd., England-RRID: SCR_015798, Guildford, Surrey, UK) and separated in KRB at 4 °C. After sectioning, three slices per well were incubated in 1 mL of KRB for 30 min, at 35 °C, for metabolic recovery before starting the experiment.

2.10.2. Cellular Viability Evaluation

Cellular viability of the hippocampal slices was determined through the reduction assay of 3-(4,5-dimethylthiazol-2-yl)-2,5-diphenyltetrazolium bromide (MTT-Sigma). Slices were quantified by measuring the reduction of MTT to dark violet formazan, a product of mitochondrial dehydrogenases. Slices were incubated with MTT (0.5 mg/mL) in a KRB buffer for 20 min at 35 °C. The medium was removed, and the precipitated formazan was solubilized with 0.2 mL of DMSO for 30 min. After the removal of slices, the resulting coloured compound was quantified by a spectrophotometer TECAN ® (Tecan Group Ltd., Mannedorf, Switzerland), equipment from the Laboratório Multiusuário de Estudos em Biologia at the Universidade Federal de Santa Catarina (LAMEB/UFSC) at a wavelength of 550 nm. Absorbance was used as an index of cellular viability [30].

2.10.3. Propidium Iodide Incorporation

Cellular membrane integrity was assessed by evaluating the incorporation of the fluorescent dye propidium iodide (PI). PI is a polar compound that enters only cells with damaged membranes. Once inside the cells, PI complexes with DNA and emits an intense fluorescence. After the recovery period, slices were incubated with 7 μg/mL of PI for 30 min at 35 °C and then washed with KRB [31]. Fluorescence was measured in a fluorescence microplate reader (TECAN®, Mannedorf, Switzerland) using 495 and 630 nm as wavelengths of excitation and emission, respectively. Results were obtained as relative fluorescence units (RFU) from individual experiments, and the RFU values were normalized by percentage relative to the control group.

2.10.4. Reactive Oxygen Species (ROS) Generation

The molecular probe 2,7-dichlorofluorescein diacetate (DCFH-DA, Sigma- Aldrich, St Louis, MO, USA) was used to measure ROS. DCFH-DA is a cell-permeable non-fluorescent probe, which is de-esterified intracellularly to the nonfluorescent form 2′,7′-dichlorofluorescein (DCFH). DCFH reacts with intracellular ROS and turns to 2′,7′-dichlorofluorescein (DCF), a highly fluorescent green die. After the recovery period, hippocampal slices were loaded with 80 μM of DCFH-DA for 30 min at 35 °C [32]. Slices were then washed with KRB and fluorescence was measured in a fluorescence microplate reader TECAN® (LAMEB/UFSC) using excitation and emission wavelengths of 480 and 525 nm, respectively. Results were obtained as relative fluorescence units (RFU) from individual experiments, and RFU values were normalized by percentage relative to the control group.

2.10.5. Mitochondrial Membrane Potential (ΔΨm) Measurement

Mitochondrial membrane potential was measured using the fluorescent probe tetramethylrhodamine ethyl ester (TMRE, Sigma-Aldrich, St Louis, MO, USA). The extinction protocol was used so that the selected concentration of TMRE, mitochondria selective fluorescent dye, was enough to form aggregates. Under these conditions, once diffused into the mitochondria, a subsequent mitochondrial depolarization results in the release of the dye, increasing the fluorescence signal. Hippocampal slices were incubated with TMRE (100 nM)

for 30 min at 35 °C [32]. Fluorescence was measured in a fluorescence microplate reader TECAN® using wavelengths of excitation and emission of 550 and 590 nm, respectively. Results were obtained as relative fluorescence units (RFU) from individual experiments, and RFU values were normalized by percentage relative to the control group.

2.10.6. L-[^{3}H]Glutamate Release

After the recovery period (30 min), hippocampal slices were incubated in Hank's balanced salt solution (HBSS), composition in millimolar: $CaCl_2$ 1.3, NaCl 137, KCl 5.36, $MgSO_4$ 0.65, Na_2HPO_4 0.3, KH_2PO_4 1.1, and HEPES 5. Glutamate uptake was assessed by adding 0.33 µCi/mL of L-[^{3}H] glutamate (American Radiolabeled Chemicals®) and 100 µM unlabelled glutamate in a final volume of 300 µL for loading the intracellular pool of L-[^{3}H]glutamate, as previously described by [33]. Glutamate uptake was stopped after 7 min at 35 °C through two washes with 1 mL of ice-cold HBSS. To induce glutamate release, slices were incubated in 300 µL of HBSS for 15 min, and the supernatant was collected to assess the amount of L-[^{3}H] glutamate release. Previous studies from our laboratory showed similar results by using D-[^{3}H] aspartate or L-[^{3}H] glutamate release [31]. Slices were homogenized by incubation with 0.1% NaOH and 0.01% SDS, and lysate aliquots were used to determine the intracellular amount of L-[^{3}H] glutamate. The intracellular and extracellular L-[^{3}H] glutamate content was analysed by the Liquid Scintillation Analyzer PerkinElmer®, and the amount of L-[^{3}H] glutamate release was expressed as a percentage of total L-[^{3}H]glutamate.

2.10.7. Protein Measurement

Protein content was evaluated by the method of Lowry et al. [34]. Bovine serum albumin 1 mg/mL (Sigma) was used as a standard.

2.11. Statistical Analysis

The normal distribution of the data was tested with the Shapiro-Wilks test, and when the distribution of the variables was normal, further analyses were carried out. Comparisons among treated and control groups were performed by two-way ANOVA, when appropriate, followed by Tukey's post hoc test. Grubb's test was used to detect outliers. The novel object recognition task was analysed by one-sample *t*-tests to determine whether the recognition index was different from 50% (random investigation). A value of $p \leq 0.05$ was considered significant. Statistical analysis and graphics were designed using GraphPad Prism® 8.0.1 software package (San Diego, CA, USA). Figures were created with BioRender.com and Servier Medical Art.

3. Results

3.1. Guanosine Prevents A$\beta_{1–42}$-Induced ROS Production

Regarding the results obtained in Protocol 1 (Figure 1A), we initially evaluated the effects of i.c.v. infusion of A$\beta_{1–42}$ and guanosine treatment on the 8th day. Mice were tested in the tail suspension test (TST) followed by the open field test (OFT) (Figure 2A,B). Two-way ANOVA revealed no alterations in the immobility time in TST ($p \geq 0.05$). However, A$\beta_{1–42}$ infusion produced an increased number of crossings in the OFT [($F_{(1,17)}$ = 7.22, (p = 0.0156)], and guanosine treatment was able to prevent this increased locomotor activity induced by A$\beta_{1–42}$ [($F_{(1,17)}$ = 4.43, (p = 0.0468)].

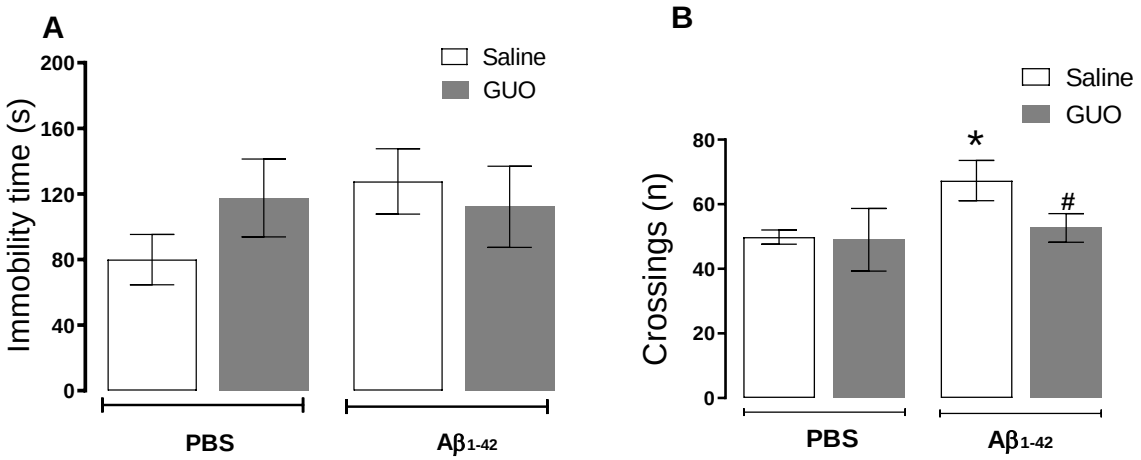

Figure 2. Evaluation of depressive-like behaviour in mice following guanosine treatment and $A\beta_{1–42}$ i.c.v. infusion. Mice subjected to $A\beta_{1–42}$ infusion (400 pmol/site, i.c.v.) received guanosine (GUO, 8 mg/kg, i.p.) for seven days. On the eighth day, mice were subjected to the tail suspension test (**A**) and to the open field test (**B**). Values expressed as mean + S.E.M (n = 6) * $p \leq 0.05$ compared with the vehicle-treated group; # $p \leq 0.05$ compared with $A\beta_{1–42}$ -treated group. (Two-way ANOVA followed by Tukey's test).

Hippocampal slices of mice subject to $A\beta_{1–42}$ infusion and guanosine (Protocol 1—Figure 1A) treatment were evaluated for ROS production and cell viability. ROS production analysis showed that vehicle-treated and guanosine-treated groups did not present any alteration in ROS production. $A\beta_{1–42}$ infusion induced a 35% increase in ROS production when compared with the vehicle-treated group [($F_{(1,15)}$ = 5.052, (p = 0.0401)], and guanosine treatment prevented this effect [($F_{(1,15)}$ = 6.165, (p = 0.0253)] (Figure 3A). Regarding hippocampal viability, both guanosine treatment and $A\beta_{1–42}$ infusion did not alter hippocampal slice viability ($p \geq 0.05$) (Figure 3B), or cellular membrane integrity ($p \geq 0.05$) (Figure 3C) at this time point.

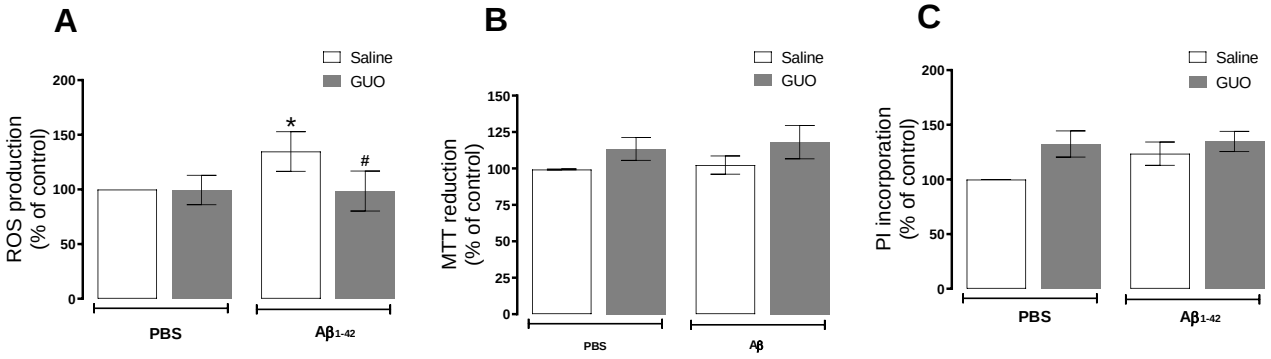

Figure 3. Guanosine prevents $A\beta_{1–42}$-induced ROS production in mice hippocampal slices. Mice subjected to i.c.v. $A\beta_{1–42}$ infusion (400 pmol/site) received guanosine (GUO, 8 mg/kg, i.p.) for seven days. On the eighth day, animals were euthanized, and hippocampal slices were analysed for ROS production (**A**), cellular viability through MTT assay (**B**), and cellular membrane damage through Propidium iodide (PI) incorporation (**C**). Values expressed as mean + S.E.M (n = 6–9) * $p \leq 0.05$ compared with vehicle-treated group. # $p < 0.05$ compared with $A\beta_{1–42}$ group. (Two-way ANOVA followed by Tukey's test).

3.2. Guanosine Prevents $A\beta_{1–42}$-Induced Short-Term Spatial Memory Impairment

As previously demonstrated by our group, $A\beta_{1–40}$ promoted an anhedonic-like behaviour and cognitive impairment [6]. Here our aim was to test $A\beta_{1–42}$ effects on these behavioural paradigms on the 10th day, as the previous protocol showed no alteration in a depressive-like behaviour assessment. Anhedonic-like behaviour was tested through

the sucrose splash test (SST) on the 10th day following treatments, as shown in the experimental design of Protocol 2 (Figure 1B). Statistical analysis indicated that $A\beta_{1–42}$ infusion and guanosine treatment (8 mg/kg—9 days) did not significantly alter both latencies to initiating the grooming behaviour ($p \geq 0.05$) and the total time of grooming ($p \geq 0.05$) (Figure 4A,B).

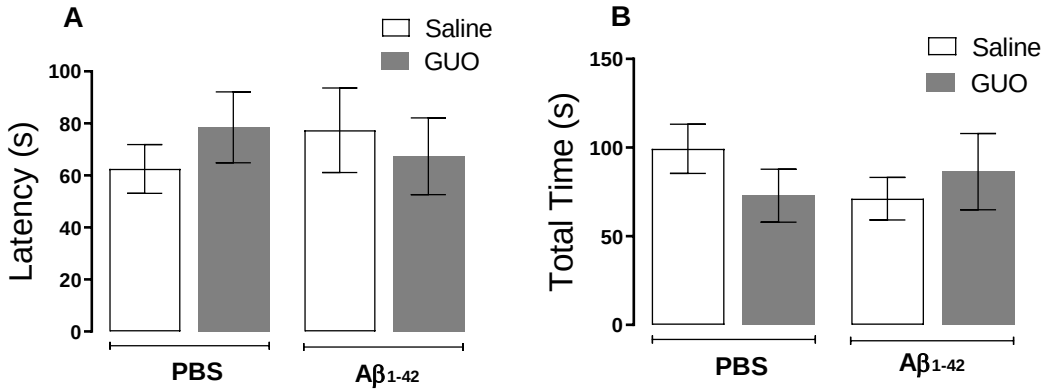

Figure 4. Evaluation of anhedonic-like behaviour in mice following guanosine treatment and $A\beta_{1–42}$ i.c.v. infusion. Mice subjected to $A\beta_{1–42}$ infusion (400 pmol/site) received guanosine (GUO, 8 mg/kg, i.p.) for nine days. On the tenth day, mice were subjected to the sucrose splash test and the latency to initiating grooming (**A**) and the total time spent in grooming activity (**B**) were measured. Values expressed as mean + S.E.M (n = 7–8). (Two-way ANOVA followed by Tukey's test).

Additionally, mouse spatial memory was analysed in the object location test (OLT). $A\beta_{1–42}$-treated mice reduced the total time of exploration of the object in a novel location (object 2) (Figure 5A). $A\beta_{1–42}$ mice displayed impaired short-term spatial memory in the OLT, observed as a decreased index of recognition of the altered object (Figure 5B). Two-way ANOVA revealed a significant difference between the control group and the $A\beta_{1–42}$ infused group [($F_{(1,32)} = 6.508$, ($p = 0.0157$)]. Guanosine treatment prevented the decreased discrimination index induced by $A\beta_{1–42}$ [($F_{(1,32)} = 4.916$, ($p = 0.0338$)], suggesting the prevention of memory impairment in this hippocampal-dependent task.

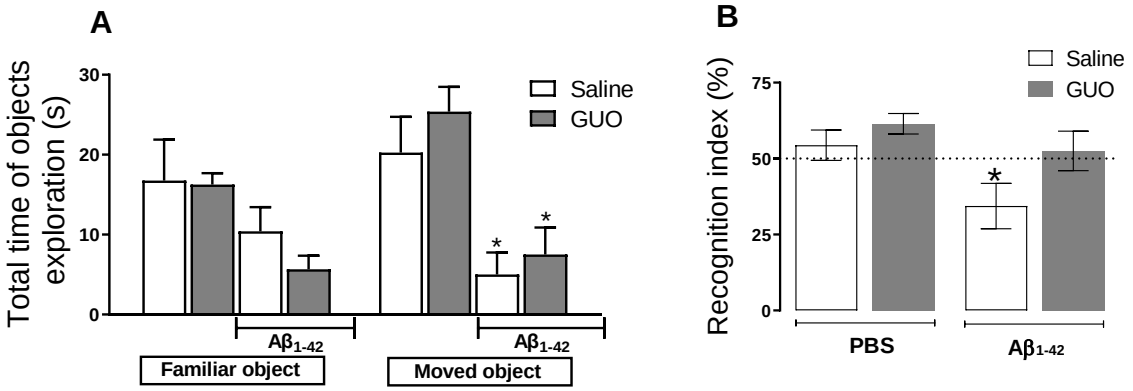

Figure 5. Guanosine prevents $A\beta_{1–42}$-induced short-term spatial memory impairment in mice. Mice subjected to $A\beta_{1–42}$ infusion (400 pmol/site) received guanosine (GUO, 8 mg/kg, i.p.) for nine days. On the tenth day, mice were subjected to the object location test and the total time of familiar and moved objects exploration were assessed (**A**) * $p \leq 0.05$ compared with the vehicle- and GUO-treated group. The recognition index of location was calculated as the percentage of time exploring the moved object in relation to the time exploring the familiar object and * $p < 0.05$ compared to the hypothetical 50 % (dashed line) of random exploration (**B**). Values expressed as mean + S.E.M (n = 8–10). (Two-way ANOVA followed by Tukey's test).

3.3. Guanosine Prevents Aβ$_{1–42}$-Induced Hippocampal Slice Damage

After behavioural analyses, an ex vivo analysis of hippocampal slices was performed by evaluating ROS production, mitochondrial membrane potential, slices cellular viability, as well as metabolic parameters (lactate and glutamate release).

Differently from the evaluation performed on the 8th day, here we observed no alteration in ROS production ($p \geq 0.05$) (Figure 6A). Additionally, no alteration in mitochondria membrane potential was observed ($p \geq 0.05$) (Figure 6B), and although not significant, glutamate release to the extracellular medium was slightly increased by Aβ$_{1–42}$ ($p = 0.1774$)] (Figure 6C). Despite the fact that the oxidative status was not altered on day 10, here we observed increased lactate levels in the superfused slices medium (as an index of glycolytic activity) [($F_{(1,18)} = 4.982$, ($p = 0.0386$)] (Figure 6D). Guanosine treatment was able to prevent this increase in lactate efflux. Slice viability analysis by MTT reduction and PI incorporation, showed decreased cell viability [($F_{(1,27)} = 3.337$, ($p = 0.0788$)] and increased membrane permeabilization [($F_{(1,29)} = 4.280$, ($p = 0.0476$)] evoked by Aβ$_{1–42}$ (Figure 7A,B), and both cell viability and [($F_{(1,27)} = 7.414$, ($p = 0.0112$)] membrane permeabilization [($F_{(1,29)} = 13.79$, ($p = 0.0009$)] were prevented by guanosine treatment, suggesting the initial ROS production was the trigger to slices alterations thereafter.

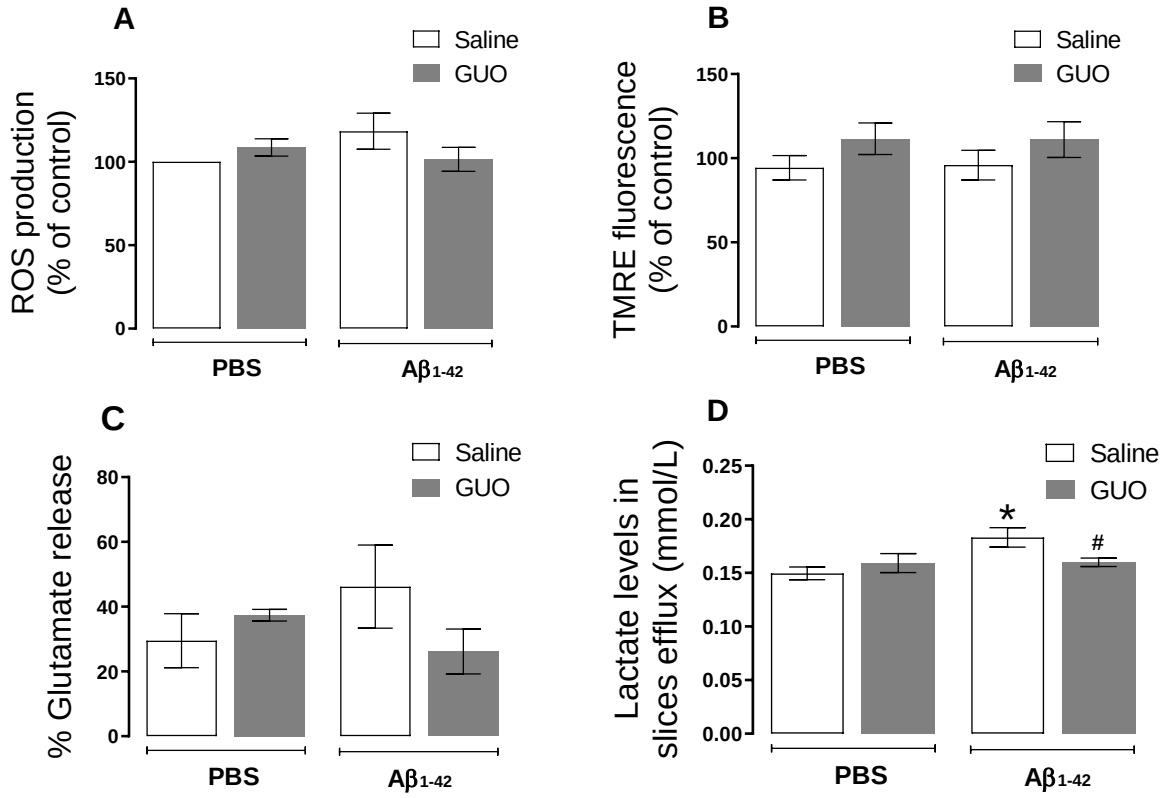

Figure 6. Biochemical evaluation of mice hippocampal slices following guanosine treatment and Aβ$_{1–42}$ i.c.v. infusion. Mice subjected to Aβ$_{1–42}$ infusion (400 pmol/site) received guanosine (GUO, 8 mg/kg, i.p.) for nine days. On the tenth day, animals were euthanized, and hippocampal slices were analyzed for ROS production (**A**), mitochondrial membrane potential through TMRE fluorescence assay (**B**), L-[^{3}H] glutamate radioactivity in slices efflux was analysed to assess glutamate release (**C**), and lactate levels in slices efflux (**D**). Values expressed as mean + S.E.M (n = 6–8) * $p \leq 0.05$ compared with vehicle-treated group. # $p < 0.05$ compared with Aβ$_{1–42}$ group. (Two-way ANOVA followed by Tukey's test).

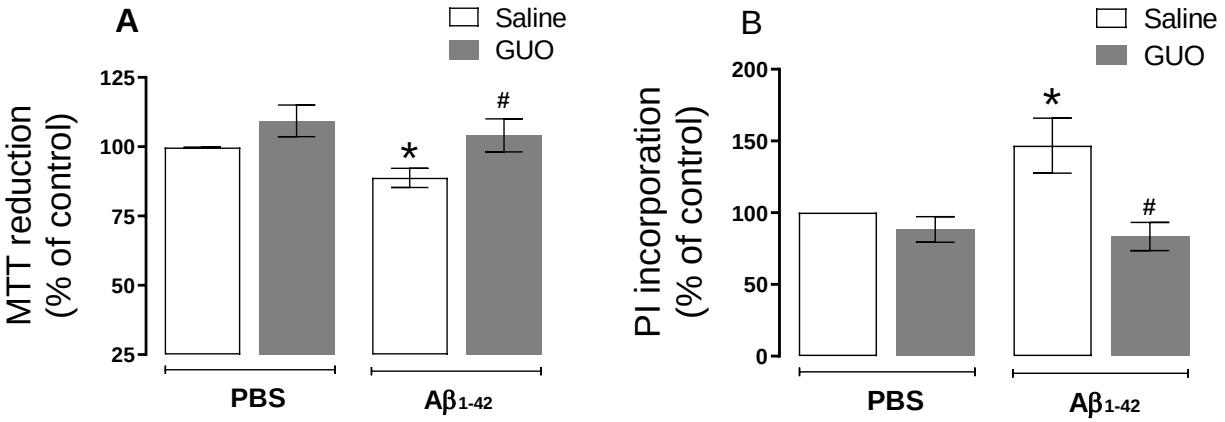

Figure 7. Guanosine prevents $A\beta_{1–42}$-induced mice hippocampal slice loos of cell viability and membrane permeabilization. Mice subjected to $A\beta_{1–42}$ infusion (400 pmol/site) received guanosine (GUO, 8 mg/kg, i.p.) for nine days. On the tenth day, animals were euthanized, and hippocampal slices were analysed for cellular viability through MTT assay (**A**), and membrane damage through PI incorporation (**B**). Values expressed as mean + S.E.M (n = 8–9) * $p \leq 0.05$ compared with vehicle-treated group. # $p < 0.05$ compared with $A\beta_{1–42}$ group. (Two-way ANOVA followed by Tukey's test).

4. Discussion

In the present study, i.c.v. infusion of $A\beta_{1–42}$ promoted impairment in short-term spatial memory in mice subjected to the object location test, a hippocampal-dependent task. Additionally, an ex vivo evaluation of hippocampal slice functionality displayed a different profile regarding slice viability, ROS production, and metabolic alterations assessed in two-time points following $A\beta_{1–42}$ infusion. The therapeutical strategy used, the intraperitoneal administration of the neuroprotective nucleoside guanosine, prevented spatial memory disruption, hippocampal ROS production, metabolic alteration, impairment in slice viability, and cell membrane damage.

The formation and aggregation of Aβ peptide oligomers are identified as the main cause of glutamatergic excitotoxicity in AD [35]. This event involves metabolic changes, inducing mitochondrial dysfunction, a process that is strongly related to the increased production of ROS, which can lead to cell death [36,37]. Whereas the administration of Aβ in the brains of rodents does not induce all the pathological aspects of AD, the intracerebroventricular (i.c.v.) infusion protocol is able to mimic the initial events of the disease, being a good model for biochemical and behavioral assessment of AD-related alterations. In the present study, we performed i.c.v. infusion of the $A\beta_{1–42}$ peptide, identified as the most abundant and neurotoxic isoform in the CNS [11].

Several studies consider oxidative stress as a crucial event in the development of AD, with increased excessive ROS production promoting Aβ deposition, tau hyperphosphorylation, and subsequently synaptic and neuronal loss [38]. Our group and other researchers previously showed an acute oxidative effect on the mouse hippocampus 24 h after $A\beta_{1–40}$ peptide i.c.v. infusion (400 pmol/site), where a significant increase in the production of ROS was observed [9,39]. Here, with i.c.v. infusion of $A\beta_{1–42}$ peptide (at the same dose used for $A\beta_{1–40}$), we also observed an increased ROS production even after seven days of $A\beta_{1–42}$ administration (Figure 3A), and such effect was no longer observed in Protocol 2, at the 10th day of treatment (Figure 6A). Meanwhile, slice viability and cell membrane integrity were not initially altered (Figure 3B,C), but they were compromised when assessed later after an $A\beta_{1–42}$ infusion (Figure 7). As previously mentioned, ROS production may be the trigger to decrease hippocampal slice viability observed thereafter.

We previously addressed the effects of $A\beta_{1–40}$ infusion in mice, showing the induction of inflammatory responses, oxidative stress, and glutamatergic transmission changes. These alterations might be associated with cognitive impairment in learning and memory

(evaluated 16 and 21 days after $A\beta_{1–40}$) [6,10]. Additionally, $A\beta_{1–40}$ promoted a reduction in hippocampal BDNF levels, and depressive-like behavior in mice (assessed ten days after $A\beta_{1–40}$) [7,8]. In the present study, where we used the $A\beta_{1–42}$ infusion, for an initial behavioral assessment, mice were subjected to TST to evaluate a depressive-like behavior and to the SST, to evaluate an anhedonic-like behaviour (Figures 2 and 4). Unlike what was observed with $A\beta_{1–40,}$ the $A\beta_{1–42}$ peptide did not significantly alter the behavior of mice in both TST and SST.

Surprisingly, $A\beta_{1–42}$ promoted an increased locomotor activity in the open field test (Figure 2B), which could resemble an anxiety-like behaviour, as shown by [40], which deserves further investigation. However, when evaluating the short-term spatial memory of mice, $A\beta_{1–42}$ evoked a reduction in the time of exploration of the object in a new location (recognition index) in the OLT (Figure 5) suggesting a memory impairment induced by $A\beta_{1–42}$. Such an effect was also previously observed with the protocol of $A\beta_{1–40}$ infusion, though it was observed after 21 days of $A\beta_{1–40}$ administration [6]. These observations point to the idea that although these different metabolic products of APP processing may have selective effects, memory impairment seems to be a similar outcome of i.c.v. administration of Aβ peptides.

A previous study from Souza da Silva et al., [23] also reported impairment in short-term memory by assessing the recognition of a novel object after 24 h, 7, and 14 days following $A\beta_{1–42}$ oligomers i.c.v. infusion. However, metabolic alterations were assessed only 48 h after $A\beta_{1–42}$ oligomers infusion and showed a partially compromised mitochondria activity. Here, on the 10th day following $A\beta_{1–42}$ i.c.v. infusion, we analyzed hippocampal slices and observed no alteration in ROS production and mitochondrial membrane potential; however, there was a tendency in increasing glutamate release, and a significantly increased content of lactate (a glycolytic product) was found in the slice supernatant (Figure 6). Glutamate measurement in the extracellular space is usually interpreted as an excitotoxicity index, but considering it is also a substrate for oxidative metabolism, increasing tricarboxylic acid cycle activity, its accumulation in the extracellular space may also be related to a decreased oxidative metabolism [41–44]. However, glutamate fate and metabolism still need clarification in this $A\beta_{1–42}$–induced toxicity protocol.

Additionally, considering the astrocytic-neuron lactate shuttle hypothesis [45], it is feasible that $A\beta_{1–42}$-induced neurotoxicity involves a metabolic shift from oxidative to glycolytic profile. However, studies in humans have shown a decreased glucose metabolism associated with amnestic mild cognitive impairment and AD-related dementia [38,46]. Therefore, a more detailed metabolomic evaluation will be further necessary to accompany Aβ-induced metabolic shifts.

The nucleoside guanosine was the therapeutic strategy used in this study since it is a neuroprotective agent known to modulate glutamate excitotoxicity [12,14], by interacting with purinergic P1 adenosine A_1/A_{2A} receptors heteromers [47], and/or calcium-activated potassium channels [48]. Guanosine was effective in preventing ROS production (Figure 3A) and increased lactate efflux (Figure 6D), and the loss of hippocampal viability (Figure 7) that accompanied memory impairment (Figure 5) in a hippocampal-dependent memory task [49,50]. Although guanosine is known to exert neuroprotection against glutamate toxicity-related disease models, such as seizures, ischemia, oxidative damage, and Parkinson's disease [14], few studies have analyzed the effects of guanosine on AD models. In vitro, SH-5YSY neuroblastoma cells showed that guanosine displayed a protective effect against ROS production and apoptotic cell death induced by Aβ [51]. In vivo, guanosine treatment prevents the cognitive deficit and anhedonic-like behavior induced by $A\beta_{1–40}$ in mice [6], and promotes presynaptic mitochondrial calcium homeostasis following $A\beta_{1–42}$ oligomers i.c.v. infusion in mice [23]. The current study was the first to evaluate guanosine protective effects following 8 to 10 days of $A\beta_{1–42}$ peptide i.c.v. infusion, the Aβ isoform most abundant in the brain and involved in triggering glutamatergic excitotoxicity and oxidative, metabolic, and behavioural distress. It is important to highlight that here guanosine did not promote any unsafe effects *per se*, and it was able to counteract the $A\beta_{1–42}$-induced

harmful behavioural and biochemical effects. Altogether, our study reinforces the neuroprotective effects of guanosine and offers some important insights into the time course of $A\beta_{1–42}$-induced neurotoxicity in the hippocampus, following i.c.v. infusion.

5. Conclusions

The present study demonstrated that guanosine prevents the initial production of ROS caused by $A\beta_{1–42}$ (following eight days of $A\beta_{1–42}$ peptide i.c.v. infusion), and is effective in preventing the damage to hippocampal slices at the same time it prevents $A\beta_{1–42}$-induced impairment of short-term spatial memory (following ten days of $A\beta_{1–42}$ peptide i.c.v. infusion). Additionally, guanosine modulates glutamate and lactate efflux from hippocampal slices (Figure 8). Overall, these findings provide support for the premise that guanosine has protective effects against memory impairment and brain damage and should be further investigated to better elucidate AD pathophysiology.

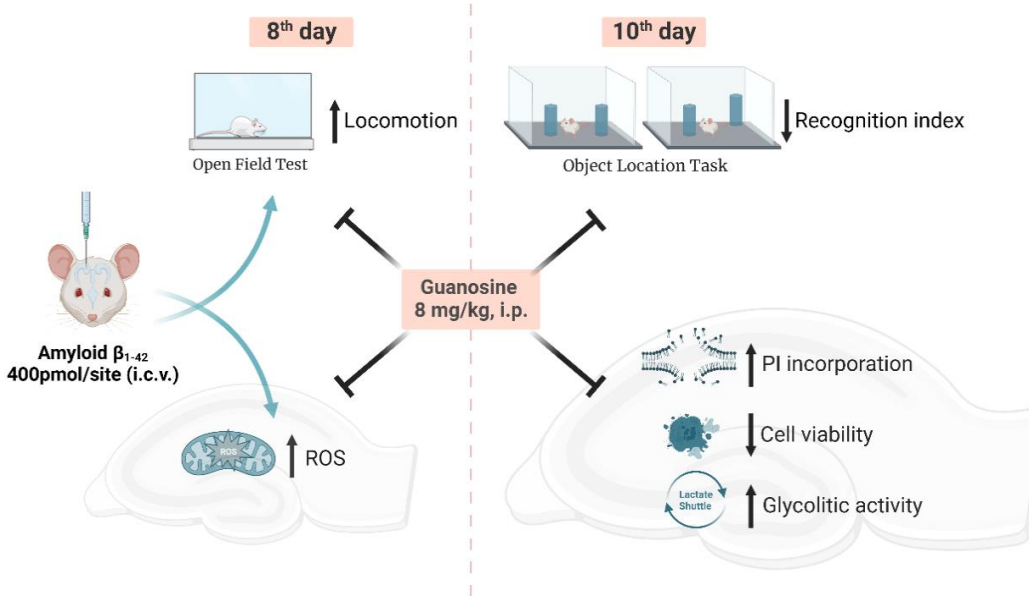

Figure 8. Schematic summary of neuroprotective effects of guanosine on behavioural and biochemical alterations in mice hippocampus following $A\beta_{1–42}$ i.c.v. infusion. Guanosine prevents alteration in the locomotor activity and the initial hippocampal ROS generation caused by $A\beta_{1–42}$ (eighth day). Guanosine is effective in preventing $A\beta_{1–42}$-induced impairment in the hippocampal-dependent short-term spatial memory and damage to hippocampal slices (tenth day). The mechanism of action of neuroprotective effect of guanosine seems to involve modulation of glutamate and lactate transport, pointing to a metabolic modulation that prevents oxidative damage.

Author Contributions: C.I.T.: conceptualization, funding acquisition, project administration, supervision, and writing. V.C.: conceptualization, data curation, formal analysis, investigation, methodology, software, and writing. L.B.B.: conceptualization, data curation, formal analysis, investigation, methodology, software, and reviewing. N.F.M.: investigation and methodology. L.C.C.: formal analysis, investigation, and methodology. G.M.: conceptualization, resources, and writing. All authors have read and agreed to the published version of the manuscript.

Funding: This study was supported by Conselho Nacional de Desenvolvimento Científico e Tecnológico (CNPq)—Instituto Nacional de Ciência e Tecnologia (INCT) for Excitotoxicity and Neuroprotection; and Coordenação de Aperfeiçoamento de Pessoal de Ensino Superior (CAPES) (CAPES-PVE 052/2012). CIT is CNPq Research Fellow. The financial support agencies had no further role in study design; in the collection, analysis, and interpretation of data; in the writing of the report; and in the decision to submit the paper for publication.

Institutional Review Board Statement: All procedures were carried out following the National Institute of Health Guide for the Care and Use of Laboratory Animals and the protocols were approved by the Institutional Ethics Committee (CEUA-UFSC-PP955).

Informed Consent Statement: Not applicable.

Data Availability Statement: All data generated or analysed during this study are included in this published article.

Conflicts of Interest: The authors declared no conflicts of interest.

References

1. Karran, E.; de Strooper, B. The Amyloid Cascade Hypothesis: Are We Poised for Success or Failure? *J. Neurochem.* **2016**, *139*, 237–252. [CrossRef] [PubMed]
2. Masters, C.L.; Bateman, R.; Blennow, K.; Rowe, C.C.; Sperling, R.A.; Cummings, J.L. Alzheimer's Disease. *Nat. Rev. Dis. Prim.* **2015**, *1*, 15056. [CrossRef] [PubMed]
3. Haass, C.; Selkoe, D.J. Soluble Protein Oligomers in Neurodegeneration: Lessons from the Alzheimer's Amyloid β-Peptide. *Nat. Rev. Mol. Cell Biol.* **2007**, *8*, 101–112. [CrossRef] [PubMed]
4. Mancini, G.; Dias, C.; Lourenço, C.F.; Laranjinha, J.; de Bem, A.; Ledo, A. A High Fat/Cholesterol Diet Recapitulates Some Alzheimer's Disease-Like Features in Mice: Focus on Hippocampal Mitochondrial Dysfunction. *J. Alzheimer's Dis.* **2021**, *82*, 1619–1633. [CrossRef] [PubMed]
5. Takeda, S.; Sato, N.; Niisato, K.; Takeuchi, D.; Kurinami, H.; Shinohara, M.; Rakugi, H.; Kano, M.; Morishita, R. Validation of Aβ1-40 Administration into Mouse Cerebroventricles as an Animal Model for Alzheimer Disease. *Brain Res.* **2009**, *1280*, 137–147. [CrossRef]
6. Lanznaster, D.; Mack, J.M.; Coelho, V.; Ganzella, M.; Almeida, R.F.; Dal-Cim, T.; Hansel, G.; Zimmer, E.R.; Souza, D.O.; Prediger, R.D.; et al. Guanosine Prevents Anhedonic-Like Behavior and Impairment in Hippocampal Glutamate Transport Following Amyloid-B1–40 Administration in Mice. *Mol. Neurobiol.* **2017**, *54*, 5482–5496. [CrossRef]
7. Ludka, F.K.; Cunha, M.P.; Dal-Cim, T.; Binder, L.B.; Constantino, L.C.; Massari, C.M.; Martins, W.C.; Rodrigues, A.L.S.; Tasca, C.I. Atorvastatin Protects from Aβ1–40-Induced Cell Damage and Depressive-Like Behavior via ProBDNF Cleavage. *Mol. Neurobiol.* **2017**, *54*, 6163–6173. [CrossRef]
8. Rosa, J.M.; Pazini, F.L.; Cunha, M.P.; Colla, A.R.S.; Manosso, L.M.; Mancini, G.; Souza, A.C.G.; de Bem, A.F.; Prediger, R.D.; Rodrigues, A.L.S. Antidepressant Effects of Creatine on Amyloid β_{1-40}-Treated Mice: The Role of GSK-3β/Nrf_2 Pathway. *Prog. Neuro-Psychopharmacol. Biol. Psychiatry* **2018**, *86*, 270–278. [CrossRef]
9. Mancini, G.; Martins, W.C.; de Oliveira, J.; de Bem, A.F.; Tasca, C.I. Atorvastatin Improves Mitochondrial Function and Prevents Oxidative Stress in Hippocampus Following Amyloid-B1–40 Intracerebroventricular Administration in Mice. *Mol. Neurobiol.* **2020**, *57*, 4187–4201. [CrossRef]
10. Piermartiri, T.C.B.; Figueiredo, C.P.; Rial, D.; Duarte, F.S.; Bezerra, S.C.; Mancini, G.; de Bem, A.F.; Prediger, R.D.S.; Tasca, C.I. Atorvastatin Prevents Hippocampal Cell Death, Neuroinflammation and Oxidative Stress Following Amyloid-B1-40 Administration in Mice: Evidence for Dissociation between Cognitive Deficits and Neuronal Damage. *Exp. Neurol.* **2010**, *226*, 274–284. [CrossRef]
11. Wang, J.; Gu, B.J.; Masters, C.L.; Wang, Y.J. A Systemic View of Alzheimer Disease—Insights from Amyloid-β Metabolism beyond the Brain. *Nat. Rev. Neurol.* **2017**, *13*, 612–623. [CrossRef] [PubMed]
12. Lanznaster, D.; Dal-Cim, T.; Piermartiri, T.C.B.; Tasca, C.I. Guanosine: A Neuromodulator with Therapeutic Potential in Brain Disorders. *Aging Dis.* **2016**, *7*, 657–679. [CrossRef] [PubMed]
13. Bettio, L.E.B.; Gil-Mohapel, J.; Rodrigues, A.L.S. Guanosine and Its Role in Neuropathologies. *Purinergic Signal.* **2016**, *12*, 411–426. [CrossRef] [PubMed]
14. Tasca, C.I.; Lanznaster, D.; Oliveira, K.A.; Fernández-Dueñas, V.; Ciruela, F. Neuromodulatory Effects of Guanine-Based Purines in Health and Disease. *Front. Cell. Neurosci.* **2018**, *12*, 376. [CrossRef]
15. Dos Santos-Rodrigues, A.; Grañé-Boladeras, N.; Bicket, A.; Coe, I.R. Nucleoside Transporters in the Purinome. *Neurochem. Int.* **2014**, *73*, 229–237. [CrossRef]
16. Zimmermann, H.; Braun, N. Extracellular Metabolism of Nucleotides in the Nervous System. *J. Auton. Pharmacol.* **1996**, *16*, 397–400. [CrossRef]
17. Ciccarelli, R.; Ballerini, P.; Sabatino, G.; Rathbone, M.P.; D'Onofrio, M.; Caciagli, F.; di Iorio, P. Involvement of Astrocytes in Purine-Mediated Reparative Processes in the Brain. *Int. J. Dev. Neurosci.* **2001**, *19*, 395–414. [CrossRef]
18. Schmidt, A.P.; Böhmer, A.E.; Schallenberger, C.; Antunes, C.; Tavares, R.G.; Wofchuk, S.T.; Elisabetsky, E.; Souza, D.O. Mechanisms Involved in the Antinociception Induced by Systemic Administration of Guanosine in Mice. *Br. J. Pharmacol.* **2010**, *159*, 1247–1263. [CrossRef]
19. Dal-Cim, T.; Poluceno, G.G.; Lanznaster, D.; de Oliveira, K.A.; Nedel, C.B.; Tasca, C.I. Guanosine Prevents Oxidative Damage and Glutamate Uptake Impairment Induced by Oxygen/Glucose Deprivation in Cortical Astrocyte Cultures: Involvement of A 1 and A 2A Adenosine Receptors and PI3K, MEK and PKC Pathways. *Purinergic Signal.* **2019**, *15*, 465–476. [CrossRef]

20. Thomaz, D.T.; Andreguetti, R.R.; Binder, L.B.; da Luz Scheffer, D.; Corrêa, A.W.; Silva, F.R.M.B.; Tasca, C.I. Guanosine Neuroprotective Action in Hippocampal Slices Subjected to Oxygen and Glucose Deprivation Restores ATP Levels, Lactate Release and Glutamate Uptake Impairment: Involvement of Nitric Oxide. *Neurochem. Res.* **2020**, *45*, 2217–2229. [CrossRef]
21. Dobrachinski, F.; Gerbatin, R.R.; Sartori, G.; Golombieski, R.M.; Antoniazzi, A.; Nogueira, C.W.; Royes, L.F.; Fighera, M.R.; Porciúncula, L.O.; Cunha, R.A.; et al. Guanosine Attenuates Behavioral Deficits After Traumatic Brain Injury by Modulation of Adenosinergic Receptors. *Mol. Neurobiol.* **2019**, *56*, 3145–3158. [CrossRef] [PubMed]
22. Courtes, A.A.; Gonçalves, D.F.; Hartmann, D.D.; da Rosa, P.C.; Cassol, G.; Royes, L.F.F.; de Carvalho, N.R.; Soares, F.A.A. Guanosine Protects against Behavioural and Mitochondrial Bioenergetic Alterations after Mild Traumatic Brain Injury. *Brain Res. Bull.* **2020**, *163*, 31–39. [CrossRef] [PubMed]
23. Da Silva, J.S.; Nonose, Y.; Rohden, F.; Lukasewicz Ferreira, P.C.; Fontella, F.U.; Rocha, A.; Brochier, A.W.; Apel, R.V.; de Lima, T.M.; Seminotti, B.; et al. Guanosine Neuroprotection of Presynaptic Mitochondrial Calcium Homeostasis in a Mouse Study with Amyloid-β Oligomers. *Mol. Neurobiol.* **2020**, *57*, 4790–4809. [CrossRef] [PubMed]
24. Rathbone, M.; Pilutti, L.; Caciagli, F.; Jiang, S. Neurotrophic Effects of Extracellular Guanosine. *Nucleosides. Nucleotides Nucleic Acids* **2008**, *27*, 666–672. [CrossRef]
25. Chojnowski, K.; Opielka, M.; Nazar, W.; Kowianski, P.; Smolenski, R.T. Neuroprotective Effects of Guanosine in Ischemic Stroke-Small Steps towards Effective Therapy. *Int. J. Mol. Sci.* **2021**, *22*, 6898. [CrossRef]
26. Piermartiri, T.C.B.; dos Santos, B.; Barros-Aragão, F.G.Q.; Prediger, R.D.; Tasca, C.I. Guanosine Promotes Proliferation in Neural Stem Cells from Hippocampus and Neurogenesis in Adult Mice. *Mol. Neurobiol.* **2020**, *57*, 3814–3826. [CrossRef]
27. Steru, L.; Chermat, R.; Thierry, B.; Simon, P. The Tail Suspension Test: A New Method for Screening Antidepressants in Mice. *Psychopharmacology* **1985**, *85*, 367–370. [CrossRef]
28. Mantovani, M.; Pértile, R.; Calixto, J.B.; Santos, A.R.S.; Rodrigues, A.L.S. Melatonin Exerts an Antidepressant-like Effect in the Tail Suspension Test in Mice: Evidence for Involvement of N-Methyl-D-Aspartate Receptors and the L-Arginine-Nitric Oxide Pathway. *Neurosci. Lett.* **2003**, *343*, 1–4. [CrossRef]
29. Rodrigues, A.L.S.; Rocha, J.B.T.; Mello, C.F.; Souza, D.O. Effect of Perinatal Lead Exposure on Rat Behaviour in Open-Field and Two-Wky Avoidance Tasks. *Pharmacol. Toxicol.* **1996**, *79*, 150–156. [CrossRef]
30. Molz, S.; Tharine, D.C.; Decker, H.; Tasca, C.I. GMP Prevents Excitotoxicity Mediated by NMDA Receptor Activation but Not by Reversal Activity of Glutamate Transporters in Rat Hippocampal Slices. *Brain Res.* **2008**, *1231*, 113–120. [CrossRef]
31. Piermartiri, T.C.B.; Vandresen-Filho, S.; de Araújo Herculano, B.; Martins, W.C.; Dal'Agnolo, D.; Stroeh, E.; Carqueja, C.L.; Boeck, C.R.; Tasca, C.I. Atorvastatin Prevents Hippocampal Cell Death Due to Quinolinic Acid-Induced Seizures in Mice by Increasing Akt Phosphorylation and Glutamate Uptake. *Neurotox. Res.* **2009**, *16*, 106–115. [CrossRef] [PubMed]
32. Dal-Cim, T.; Ludka, F.K.; Martins, W.C.; Reginato, C.; Parada, E.; Egea, J.; Lõpez, M.G.; Tasca, C.I. Guanosine Controls Inflammatory Pathways to Afford Neuroprotection of Hippocampal Slices under Oxygen and Glucose Deprivation Conditions. *J. Neurochem.* **2013**, *126*, 437–450. [CrossRef] [PubMed]
33. Molz, S.; Dal-Cim, T.; Budni, J.; Martín-de-Saavedra, M.D.; Egea, J.; Romero, A.; del Barrio, L.; Rodrigues, A.L.S.; López, M.G.; Tasca, C.I. Neuroprotective Effect of Guanosine against Glutamate-Induced Cell Death in Rat Hippocampal Slices Is Mediated by the Phosphatidylinositol-3 Kinase/Akt/Glycogen Synthase Kinase 3β Pathway Activation and Inducible Nitric Oxide Synthase Inhibition. *J. Neurosci. Res.* **2011**, *89*, 1400–1408. [CrossRef] [PubMed]
34. Lowry, O.H.; Rosebrough, N.J.; Farr, A.L.; Randall, R.J. Protein Measurement with the Folin Phenol Reagent. *J. Biol. Chem.* **1951**, *193*, 265–275. [CrossRef]
35. Findley, C.A.; Bartke, A.; Hascup, K.N.; Hascup, E.R. Amyloid Beta-Related Alterations to Glutamate Signaling Dynamics During Alzheimer's Disease Progression. *ASN Neuro* **2019**, *11*, 1759091419855541. [CrossRef]
36. Tait, S.W.G.; Green, D.R. Mitochondria and Cell Signalling. *J. Cell Sci.* **2012**, *125*, 807–815. [CrossRef]
37. Stowe, D.F.; Camara, A.K.S. Mitochondrial Reactive Oxygen Species Production in Excitable Cells: Modulators of Mitochondrial and Cell Function. *Antioxid. Redox Signal.* **2009**, *11*, 1373–1414. [CrossRef]
38. Butterfield, D.A.; Halliwell, B. Oxidative Stress, Dysfunctional Glucose Metabolism and Alzheimer Disease. *Nat. Rev. Neurosci.* **2019**, *20*, 148–160. [CrossRef]
39. Bicca, M.A.; Figueiredo, C.P.; Piermartiri, T.C.; Meotti, F.C.; Bouzon, Z.L.; Tasca, C.I.; Medeiros, R.; Calixto, J.B. The Selective and Competitive N-Methyl-D-Aspartate Receptor Antagonist, (-)-6-Phosphonomethyl-Deca-Hydroisoquinoline-3-Carboxylic Acid, Prevents Synaptic Toxicity Induced by Amyloid-β in Mice. *Neuroscience* **2011**, *192*, 631–641. [CrossRef]
40. Souza, L.C.; Jesse, C.R.; Antunes, M.S.; Ruff, J.R.; de Oliveira Espinosa, D.; Gomes, N.S.; Donato, F.; Giacomeli, R.; Boeira, S.P. Indoleamine-2,3-Dioxygenase Mediates Neurobehavioral Alterations Induced by an Intracerebroventricular Injection of Amyloid-B1-42 Peptide in Mice. *Brain. Behav. Immun.* **2016**, *56*, 363–377. [CrossRef]
41. Sonnewald, U.; Westergaard, N.; Schousboe, A. Glutamate Transport and Metabolism in Astrocytes. *Glia* **1997**, *21*, 56–63. [CrossRef]
42. McKenna, M.C.; Sonnewald, U.; Huang, X.; Stevenson, J.; Zielke, H.R. Exogenous Glutamate Concentration Regulates the Metabolic Fate of Glutamate in Astrocytes. *J. Neurochem.* **1996**, *66*, 386–393. [CrossRef] [PubMed]
43. Whitelaw, B.S.; Robinson, M.B. Inhibitors of Glutamate Dehydrogenase Block Sodium-Dependent Glutamate Uptake in Rat Brain Membranes. *Front. Endocrinol.* **2013**, *4*, 123. [CrossRef] [PubMed]

44. Mahmoud, S.; Gharagozloo, M.; Simard, C.; Gris, D. Astrocytes Maintain Glutamate Homeostasis in the CNS by Controlling the Balance between Glutamate Uptake and Release. *Cells* **2019**, *8*, 184. [CrossRef] [PubMed]
45. Pellerin, L.; Magistretti, P.J. Glutamate Uptake into Astrocytes Stimulates Aerobic Glycolysis: A Mechanism Coupling Neuronal Activity to Glucose Utilization. *Proc. Natl. Acad. Sci. USA* **1994**, *91*, 10625–10629. [CrossRef]
46. Gordon, B.A.; Blazey, T.M.; Su, Y.; Hari-Raj, A.; Dincer, A.; Flores, S.; Christensen, J.; McDade, E.; Wang, G.; Xiong, C.; et al. Spatial Patterns of Neuroimaging Biomarker Change in Individuals from Families with Autosomal Dominant Alzheimer's Disease: A Longitudinal Study. *Lancet. Neurol.* **2018**, *17*, 241–250. [CrossRef]
47. Lanznaster, D.; Massari, C.M.; Marková, V.; Šimková, T.; Duroux, R.; Jacobson, K.A.; Fernández-Dueñas, V.; Tasca, C.I.; Ciruela, F. Adenosine A_1–A_{2A} Receptor-Receptor Interaction: Contribution to Guanosine-Mediated Effects. *Cells* **2019**, *8*, 1630. [CrossRef]
48. Dal-Cim, T.; Martins, W.C.; Santos, A.R.S.; Tasca, C.I. Guanosine Is Neuroprotective against Oxygen/Glucose Deprivation in Hippocampal Slices via Large Conductance Ca^{2+}-Activated K^+ Channels, Phosphatidilinositol-3 Kinase/Protein Kinase B Pathway Activation and Glutamate Uptake. *Neuroscience* **2011**, *183*, 212–220. [CrossRef]
49. Vogel-Ciernia, A.; Wood, M.A. Examining Object Location and Object Recognition Memory in Mice. *Curr. Protoc. Neurosci.* **2014**, *69*, 8.31.1–8.31.17. [CrossRef]
50. Denninger, J.K.; Smith, B.M.; Kirby, E.D. Novel Object Recognition and Object Location Behavioral Testing in Mice on a Budget. *J. Vis. Exp.* **2018**, *2018*, e58593. [CrossRef]
51. Tarozzi, A.; Bartolini, M.; Piazzi, L.; Valgimigli, L.; Amorati, R.; Bolondi, C.; Djemil, A.; Mancini, F.; Andrisano, V.; Rampa, A. From the Dual Function Lead AP2238 to AP2469, a Multi-Target-Directed Ligand for the Treatment of Alzheimer's Disease. *Pharmacol. Res. Perspect.* **2014**, *2*, 23. [CrossRef] [PubMed]